Determination of the elastic parameters of layered weakly anisotropic media using traveltimes and polarizations

S. M. Soukina, D. Gajewski, and B. M. Kashtan

email: *soukina@dkrz.de*

keywords: *weak anisotropy, inversion, quasi-shear waves, traveltimes, polarization*

ABSTRACT

An inversion procedure for weakly anisotropic media with arbitrary symmetry is developed. The assumption of weak anisotropy allows to simplify the solution of the forward modeling and to obtain linear relations between perturbations of the elastic parameters with respect to an isotropic background medium and the corresponding traveltime perturbations. The relations are inherently linear for qP-wave traveltimes, and can be linearized for qS-wave traveltimes using the qS-wave polarization vectors. These vectors are available from a seismic experiment as well as traveltimes. Based on these linear relations the same linear inversion scheme is applied for qP- as well as for qS-wave data. The joint inversion of qP- and qS-waves allows to determine the full elastic tensor of the anisotropic medium. The inversion procedure can be applied to determine the elastic parameters of layered weakly anisotropic media. The inversion is performed by a layer-by-layer manner. The inversion procedure is tested using synthetic noise-free and noisy data for a layered model.

INTRODUCTION

The goal of inversion in the presence of anisotropy is the determination of the elastic parameters from observed seismograms. The perturbation method is used for the computation of traveltimes in the anisotropic medium. The traveltime of each wave propagating in the anisotropic medium is represented as a sum of the traveltime in the isotropic background medium and the traveltime perturbation due to the deviation of the elastic parameters of the anisotropic medium from the isotropic ones. The basic relations for traveltime perturbations in weakly anisotropic media were established in 1982 (see, e.g. Červený, 1982). In the homogeneous case the qP-wave traveltime perturbations $\Delta\tau_{qP}$ due to the perturbations of the elastic parameters Δa_{iklm} read as follows (see, e.g., Jech and Pšenčík, 1989):

$$\Delta\tau_{qP} = -\frac{\tau_p}{2}\Delta a_{iklm}\, p_i\, p_m\, n_k\, n_l. \tag{1}$$

Throughout this article summation over the repeated indices is assumed. Here, p_i and τ_p are the components of the slowness vector and the traveltime of the P-wave, respectively, in the isotropic background medium, and n_k are components of the P-wave normal vector. In isotropic media the normal vector $\mathbf{n}$ coincides with the P-wave polarization vector. With the known isotropic background medium, the traveltime τ_p and the vectors $\mathbf{p}$ and $\mathbf{n}$ can be calculated by the standard isotropic ray method. As a result, equation (1) provides a linear relation between the perturbations of the elastic parameters Δa_{iklm} and the traveltime perturbations $\Delta\tau_{qP}$. Therefore, to determine Δa_{iklm} a conventional tomography scheme can be applied.

Application of equation (1) for inversion of the elastic parameters of an anisotropic medium was considered by Chapman and Pratt (1992). They inverted the elastic parameters of arbitrary anisotropic media from qP-wave traveltime observations in a 2-D cross-borehole tomographic experiments (i.e., the rays remain in a 2-D plane containing the borehole). Of course, only a restricted number of the elastic parameters can be determined in the 2-D experiments.

For quasi-shear waves the relations between the traveltime perturbations $\Delta\tau_{qSM}$ and the perturbations Δa_{iklm} of the elastic parameters

$$\Delta\tau_{qSM} = -\frac{\tau_s}{2}\Delta a_{iklm}\, p_i\, p_m\, \mathrm{g}_k^{(M)}\, \mathrm{g}_l^{(M)}, \qquad M = 1, 2 \tag{2}$$

are intrinsically more complicated than for the quasi-compressional waves. First, there are two qS-waves: indices $M = 1$ and 2 correspond to $qS1$- and $qS2$-waves. The structure of equations (1) and (2) is similar: t_s and p_i are the traveltime and the slowness components of the S-wave, respectively, and $\mathrm{g}_k^{(M)}$ can be considered as components of the polarization vector of the S-wave in the isotropic background medium (similar to vector $\mathbf{n}$ which can be considered as the P-wave polarization vector). The second problem is related to the components n_k which are known in the isotropic background medium, whereas $\mathrm{g}_k^{(M)}$ are not. The vectors $\mathbf{g}^{(M)}$ depend on the perturbations of the elastic parameters Δa_{iklm}. Therefore, they can not be obtained until the perturbations Δa_{iklm} are known. This leads to a non-linear behavior of the qS-wave traveltime perturbations with respect to the perturbation of the elastic parameters. Červený and Jech (1982) suggested linearized equations for quasi-shear waves based on an average value of the traveltime corrections for both quasi-shear waves. Jech and Pšenčík (1992) performed a simultaneous inversion for qP- and qS-waves, but the inversion scheme can only be applied to TI structure.

We suggest to use the observed qS-wave polarization vectors to estimate the unknown vectors $\mathbf{g}^{(M)}$. With the known vectors $\mathbf{g}^{(M)}$ relations (2) is linear and formally identical to relation (1) for qP-waves. This would allow to use the same inversion scheme for qP- as for qS-waves.

Observations of qS-wave polarization vectors are available from three-component seismograms as well as traveltimes. The polarization data can be used to invert for medium parameters or to improve the resolution of the tomographic image. Several papers using the polarization for tomography have been published. For instance, Le Bégat and Farra (1997) inverted qP-wave traveltimes and polarizations of synthetic examples simulating a VSP experiment. Horne and Leaney (2000) inverted qP- and qSV polarization and slowness component measurements obtained from a walk-away VSP experiment using a global optimization method. Horne and MacBeth (1994) developed a genetic algorithm to invert shear-wave observations from VSP data. They used horizontal polarizations and time-delays between two qS-waves to invert for hexagonal and orthorombic symmetry. Farra and Le Bégat (1995) investigated the sensitivity of qP-wave traveltime and polarization vectors to heterogeneity, anisotropy and interfaces.

Borehole seismic data have traditionally been analyzed by inverting traveltimes for velocity structure. The down-hole and cross-hole experiments are ideal for determining seismic anisotropy (see, e.g., Cliet et al., 1991; Williamson, 1993). The angular coverage makes the seismic traveltimes sensitive to any type of anisotropy. In this study, a vertical seismic profiling (VSP) experiment is considered. Wavefields from sources distributed on the Earth's surface are recorded at receivers within a vertical borehole. Traveltimes of transmitted qP- and qS-waves are inverted to determine the elastic parameters of the anisotropic medium between the sources and receivers. We present a joint inversion of qP- and qS-waves in piecewise homogeneous weakly anisotropic media using a linear inversion formalism for both qP- and qS-waves. Similar to previous studies, we assume that each of the two propagating qS-waves are recorded separately, i.e., no qS-wave coupling exists, and that the observations are not close to singular directions.

After this introduction a discussion of the linearized equations for the qS-waves follows. Special emphasis is given to the determination of the vectors $\mathbf{g}^{(M)}$ for the inversion using the observed polarization vectors of qS-waves. Following this, the tomographic system is presented. Then, a numerical case study demonstrates the applicability of the inversion scheme for a layered model.

LINEARIZED EQUATIONS FOR qS-WAVE TRAVELTIME PERTURBATIONS

Since the qP- and qS-wave traveltimes in the weakly anisotropic medium are represented as $\tau_{qP} = \tau_p + \Delta\tau_{qP}$, $\tau_{qS1} = \tau_s + \Delta\tau_{qS1}$ and $\tau_{qS2} = \tau_s + \Delta\tau_{qS2}$, equations (1) and (2) can also be written in the form:

$$\begin{aligned} \tau_{qP} - \tau_p &= -\frac{\tau_p}{2}\,\Delta a_{iklm}\, p_i\, p_m\, n_k\, n_l, \\ \tau_{qSM} - \tau_s &= -\frac{\tau_s}{2}\,\Delta a_{iklm}\, p_i\, p_m\, \mathrm{g}_k^{(M)}\, \mathrm{g}_l^{(M)}, \quad M = 1, 2. \end{aligned} \tag{3}$$

The structure of all equations (3) is similar: τ_{qP}, τ_{qS1} and τ_{qS2} are the traveltimes of the qP- and qS-waves in the weakly anisotropic medium, τ_p and τ_s are the traveltimes of P- and S-waves, p_i are components the P- or S-wave slowness, and n_k are components of the wavefront normal vector in the isotropic background medium. The wavefront normal vector can also be considered as the P-wave polarization vector. The components $g_k^{(M)}$ ($M = 1$ or 2) define the vectors $\mathbf{g}^{(M)}$ introduced into the perturbation theory (see, e.g., Jech and Pšenčík, 1989; Červený, 2001). They are situated into the plane perpendicular to the ray in the isotropic background medium, and, therefore, can be considered as vectors determining S-wave polarization vectors.

The traveltimes in the weakly anisotropic medium τ_{qP}, τ_{qS1}, and τ_{qS2} are supposed to be obtained by observations. With the known parameters of the isotropic background medium, the traveltimes τ_p and τ_s, the slowness vectors of the P- and S-waves and the wavefront normal $\mathbf{n}$ can be calculated by standard isotropic ray method. As a result, in the case of qP-waves, the traveltime perturbation $\tau_{qP} - \tau_p$ and the perturbations of the elastic parameters Δa_{iklm} are linearly related. In the case of qS-waves, the vectors $\mathbf{g}^{(1)}$ and $\mathbf{g}^{(2)}$ depend on the perturbations Δa_{iklm} and, therefore, can not be determined until the perturbations Δa_{iklm} are known. This leads to a non-linear behavior of the qS-wave traveltime perturbation with respect to the perturbation of the elastic parameters Δa_{iklm}. If the vectors $\mathbf{g}^{(1)}$ and $\mathbf{g}^{(2)}$ were known, the relations between the traveltime perturbations $\tau_{qS1} - \tau_s$ or $\tau_{qS2} - \tau_s$ and the perturbations Δa_{iklm} of the elastic parameters become linear and formally identical to the relations for qP-waves.

How can we find or estimate the vectors $\mathbf{g}^{(1)}$ and $\mathbf{g}^{(2)}$ without a priori knowledge about Δa_{iklm}? For this purpose, let us consider the physical meaning of these vectors. The vectors $\mathbf{g}^{(1)}$ and $\mathbf{g}^{(2)}$ are mutually orthogonal and situated in the plane orthogonal to the ray in the isotropic background medium. For brevity, we will denote this ray reference ray. These vectors can be considered as polarization vectors of the shear-waves propagating in the isotropic background medium along the reference ray. Since the isotropic medium itself does not fix the polarization of the shear-wave, it can be described by any unit vector in the plane orthogonal to the ray. In perturbation theory, however, the specification of the vectors $\mathbf{g}^{(1)}$ and $\mathbf{g}^{(2)}$ is unique. It is controlled by the perturbations Δa_{iklm}. Thus, we get different vectors $\mathbf{g}^{(M)}$ for different Δa_{iklm}. Contrary to isotropic media, any anisotropic medium uniquely fixes the qS-wave polarizations (with exception of so-called singular directions). To provide a continuous and smooth transformation from isotropy to anisotropy, the vectors $\mathbf{g}^{(1)}$ and $\mathbf{g}^{(2)}$ must also be close to the qS-wave polarization vectors in the weakly anisotropic medium. Using this reasoning, we suggest to determine the unknown vectors $\mathbf{g}^{(1)}$ and $\mathbf{g}^{(2)}$ from the observed qS-wave polarization vectors.

The qS-wave polarization vectors are available from the experiment as well as traveltimes. Usually, to obtain traveltimes, the two qS-waves should be separated by some processing. For this separation the difference in qS-wave polarizations is used (see, e.g., Alford, 1986; Li and Crampin, 1993; Dellinger et al., 1998). Therefore, the qS-wave polarization vectors are automatically obtained as a by-product of the qS-wave separation.

To determine the vectors $\mathbf{g}^{(1)}$ and $\mathbf{g}^{(2)}$ from the observed qS-wave polarization vectors, the following procedure is performed (see Fig. 1*a*): Let us assume that at a receiver point observations of two polarization vectors $\mathbf{A}_{qS1}$ and $\mathbf{A}_{qS2}$ are available. First, the reference ray in the isotropic background medium connecting the source and the receiver is calculated. The determination of the reference medium is discussed below. Then, at the receiver point, a plane orthogonal to the reference ray is constructed. The observed

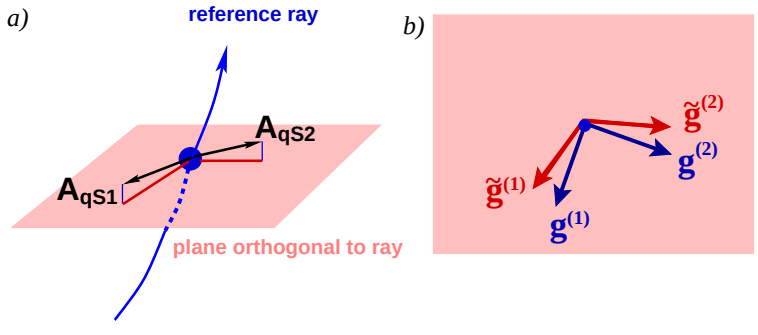

Figure 1: Estimation of the vectors $\mathbf{g}^{(1)}$ and $\mathbf{g}^{(2)}$. The observed qS-wave polarization vectors $\mathbf{A}_{qS1}$ and $\mathbf{A}_{qS2}$ are projected onto the plane orthogonal to the reference ray *(a)*. The unit vectors corresponding to the projections are denoted by $\tilde{\mathbf{g}}^{(1)}$ and $\tilde{\mathbf{g}}^{(2)}$ *(b)*. These vectors are used in eqs. (3) instead of the unknown vectors $\mathbf{g}^{(1)}$ and $\mathbf{g}^{(2)}$.

polarization vectors $\mathbf{A}_{qS1}$ and $\mathbf{A}_{qS2}$ are projected onto this plane and their projections are normalized to unit vectors. The normalized projections will be denoted as $\tilde{\mathbf{g}}^{(1)}$ and $\tilde{\mathbf{g}}^{(2)}$. Although these vectors $\tilde{\mathbf{g}}^{(1)}$ and $\tilde{\mathbf{g}}^{(2)}$ are usually not orthogonal, we suggest to use them in equations (3) instead of the unknown vectors $\mathbf{g}^{(1)}$ and $\mathbf{g}^{(2)}$ (see Fig. 1*b*). The accuracy of this approximation is investigated below.

As a result, the tomographic system is now composed by the following equations which contain the vectors $\tilde{\mathbf{g}}^{(1)}$ and $\tilde{\mathbf{g}}^{(2)}$ instead of $\mathbf{g}^{(1)}$ and $\mathbf{g}^{(2)}$:

$$\begin{aligned} \frac{\tau_{qP}}{\tau_p} - 1 &= -\frac{1}{2}\; p_i\; p_m\; n_k\; n_l \quad \Delta a_{iklm}, \\ \underbrace{\frac{\tau_{qSM}}{\tau_s} - 1}_{y_i} &= \underbrace{-\frac{1}{2}\; p_i\, p_m\, \tilde{\mathrm{g}}_k^{(M)}\, \tilde{\mathrm{g}}_l^{(M)}}_{X_{ik}}\; \underbrace{\Delta a_{iklm}}_{a_k}, \qquad M = 1, 2, \end{aligned} \tag{4}$$

where the traveltimes τ_{qP}, τ_{qS1}, τ_{qS2} and the vectors $\tilde{\mathbf{g}}^{(1)}$ and $\tilde{\mathbf{g}}^{(2)}$ are obtained by observations. The brackets are explained in the next section. For the given isotropic background medium equations (4) provide linear relations between the traveltime perturbations and the perturbation of the elastic parameters for both types of waves.

INVERSION

Let us assume that there are N observations of qP- and qS-wave traveltimes $\tau_1, \tau_2, \ldots, \tau_N$ in a weakly anisotropic medium. Each t_i corresponds to τ_{qP}, τ_{qS1} or τ_{qS2}. Based on these observations, the tomographic system is constructed from equations (4). Each traveltime τ_i for either qP- or qS-waves adds a corresponding equation in the tomography system. The system can be written in the form (see also the brackets in eqs. 4):

$$y_i = \sum_{k=1}^{L} X_{ik}\, a_k \qquad (i = 1, \ldots N, \quad N > L), \tag{5}$$

where the vector $\mathbf{y}$ is specified as $y_i = \dfrac{\tau_i}{\tau_i^{(0)}} - 1$. The components y_i are formed by the traveltimes τ_i of the qP- and qS-waves and the corresponding traveltimes $\tau_i^{(0)}$ of the P- and S-waves in the isotropic background medium. The vector $\mathbf{y}$ has a dimension N of the total number of the qP- and qS-wave traveltime observations for all receivers from all sources. The vector $\mathbf{a}$ of the perturbations Δa_{iklm} of the elastic parameters has the dimension L. The maximum value of L is equal to 21. The value of L can be reduced. For example, if the anisotropic medium under consideration is transversely isotropic, L is equal to 5. The elements of the $N \times L$ matrix $\mathbf{X}$ are composed by components of the P- or S-wave slowness vectors and the vectors $\mathbf{n}$, $\tilde{\mathbf{g}}^{(1)}$ or $\tilde{\mathbf{g}}^{(2)}$. As soon as the reference ray connecting a source and a receiver is constructed, the corresponding element of the matrix $\mathbf{X}$ can be obtained according to eqution (4).

The system of equations (5) is solved by the minimizing the misfit function η^2 (Linnik, 1961)

$$\eta^2 = \sum_{i=1}^{N} \left[\tau_i^{(0)}\right]^2 \left(y_i - \sum_{k=1}^{L} X_{ik}\, a_k \right)^2 . \tag{6}$$

The singular value decomposition (SVD) method is used for the minimization (see e.g. Menke, 1984).

DETERMINATION OF THE ISOTROPIC BACKGROUND MEDIUM

The inverse problem discussed is linear only if the isotropic background medium is known. With an unknown background medium the inversion is non-linear for qP- as well as for qS-waves. In general, the isotropic background medium is unknown as well. We can only make assumptions about the background medium. To overcome this problem the inversion procedure is embedded into an iteration procedure for the determination of the isotropic background medium. Properties of the isotropic background medium are specified by the velocities v_p and v_s of the P- and S-waves propagating in the homogeneous isotropic medium. First, the initial velocities $v_p^{(0)}$ and $v_s^{(0)}$ are defined. For example, they can be estimated for several

source-receiver pairs as the distance divided by the corresponding traveltimes. In the next step the elastic parameters of the anisotropic medium are determined by the inversion using the isotropic background medium defined by $v_p^{(0)}$ and $v_s^{(0)}$. Then, the inverted elastic parameters of the anisotropic medium are used to construct an updated isotropic background model $v_p^{(\mathrm{new})}$ and $v_s^{(\mathrm{new})}$ using the formulae for the best-fitting isotropic medium derived by Fedorov (1968). The inversion and update of the isotropic background are repeated until the old velocities and the new velocities of the isotropic background differ only by a small value (e.g., 0.01 km/s).

ACCURACY OF VECTORS $\tilde{\mathbf{g}}^{(1)}$ AND $\tilde{\mathbf{g}}^{(2)}$

In this section we investigate how close the vectors $\tilde{\mathbf{g}}^{(1)}$ and $\tilde{\mathbf{g}}^{(2)}$ estimated from the qS-wave polarization vectors, $\mathbf{A}_{qS1}$ and $\mathbf{A}_{qS2}$, are to the vectors $\mathbf{g}^{(1)}$ and $\mathbf{g}^{(2)}$ (we will call these vectors as exact vectors). For this purpose, the angles, $\tilde{\alpha}_1$ and $\tilde{\alpha}_2$, between the exact and estimated vectors are calculated (see Fig. 1*b*):

$$\tilde{\alpha}_1 = \angle(\tilde{\mathbf{g}}^{(1)}, \mathbf{g}^{(1)}), \qquad \tilde{\alpha}_2 = \angle(\tilde{\mathbf{g}}^{(2)}, \mathbf{g}^{(2)}). \tag{7}$$

For comparison also the angles between the vectors $\mathbf{A}_{qS1}$ and $\mathbf{A}_{qS2}$, and the corresponding vectors $\mathbf{g}^{(1)}$ and $\mathbf{g}^{(2)}$ derived from the perturbation theory are computed:

$$\alpha_1 = \angle(\mathbf{A}_{qS1}, \mathbf{g}^{(1)}), \qquad \alpha_2 = \angle(\mathbf{A}_{qS2}, \mathbf{g}^{(2)}). \tag{8}$$

Calculations of the angles (7) and (8) are carried out for three homogeneous anisotropic media: an orthorombic medium with 10.6% relative mean square (RMS) deviation from isotropy and a VTI medium with 11% RMS deviation from isotropy (Thomsen parameters: $\varepsilon = 0.125$, $\gamma = 0.049$ and $\delta = 0.045$). The elastic parameters of the orthorombic and VTI media are given in Table 1 (see columns with A_{ik}^{true}).

The angles are computed for different ray directions defined by an inclination angle θ and an azimuth angle φ. Each pair (θ, φ) defines a ray connecting a source and a receiver. The $qS1$- and $qS2$-waves propagating along this ray are considered. The qS-wave polarization vectors $\mathbf{A}_{qS1}$ and $\mathbf{A}_{qS2}$ at the receiver are calculated by standard anisotropic ray theory.

The vectors $\mathbf{A}_{qS1}$ and $\mathbf{A}_{qS2}$ are considered as observed qS-wave polarization data and are used for the estimation of the vectors $\tilde{\mathbf{g}}^{(1)}$ and $\tilde{\mathbf{g}}^{(2)}$. The background isotropic medium is constructed as a best-fitting

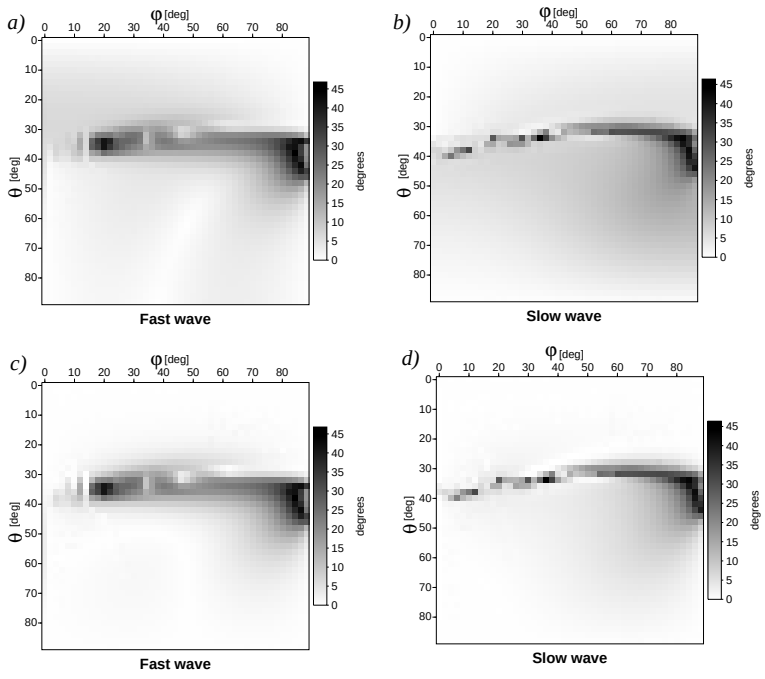

Figure 2: Maps of angles α_1, α_2, $\tilde{\alpha}_1$ and $\tilde{\alpha}_2$ (for determination of angles see text) in the orthorombic medium from Tab. 1*a*. The inclination angle θ and azimuth angle φ define the ray direction. The two upper maps, *(a)* and *(b)*, represent the angles α_1 and α_2 between the vectors $\mathbf{g}^{(1)}$ and $\mathbf{g}^{(2)}$ obtained from perturbation theory and the polarization vectors of the two qS-waves $\mathbf{A}_{qS1}$ and $\mathbf{A}_{qS2}$ computed by standard anisotropic ray theory. The two lower maps, *(c)* and *(d)*, represent the angles $\tilde{\alpha}_1$ and $\tilde{\alpha}_2$ between the vectors $\mathbf{g}^{(1)}$ and $\mathbf{g}^{(2)}$ and the vectors $\tilde{\mathbf{g}}^{(1)}$ and $\tilde{\mathbf{g}}^{(2)}$ estimated from $\mathbf{A}_{qS1}$ and $\mathbf{A}_{qS2}$. Note that the regions with the largest angles (dark) correspond to singular regions in the orthorombic medium.

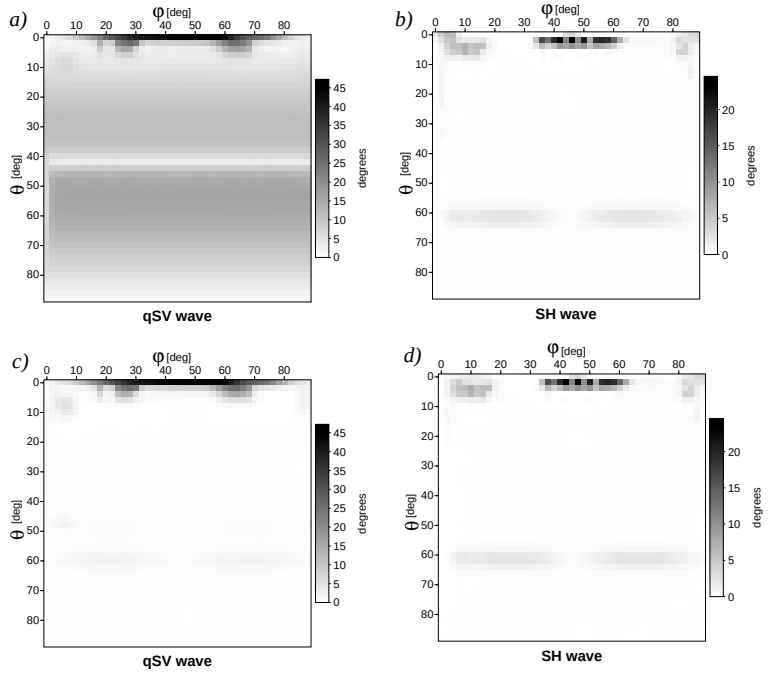

Figure 3: Maps of angles α_1, α_2, $\tilde{\alpha}_1$ and $\tilde{\alpha}_2$ in the VTI medium from Tab. 1*b*. The inclination angle θ and azimuth angle φ define the ray direction. The two upper maps, *(a)* and *(b)*, represent the angles α_1 and α_2 between the vectors $\mathbf{g}^{(1)}$ and $\mathbf{g}^{(2)}$ obtained from perturbation theory and the polarization vectors of the two qS-waves $\mathbf{A}_{qSV}$ and $\mathbf{A}_{SH}$ computed by standard anisotropic ray theory. The two lower maps, *(c)* and *(d)*, represent the angles $\tilde{\alpha}_1$ and $\tilde{\alpha}_2$ between the vectors $\mathbf{g}^{(1)}$ and $\mathbf{g}^{(2)}$ and the vectors $\tilde{\mathbf{g}}^{(1)}$ and $\tilde{\mathbf{g}}^{(2)}$ estimated from $\mathbf{A}_{qSV}$ and $\mathbf{A}_{SH}$. Note that the regions with the largest angles (dark) correspond to singular regions in the VTI medium.

isotropic medium. In the homogeneous case, the reference ray in the isotropic background medium is a straight line connecting the source and the receiver. The vectors $\mathbf{A}_{qS1}$ and $\mathbf{A}_{qS2}$ are projected onto a plane perpendicular to the reference ray. The exact vectors $\mathbf{g}^{(1)}$ and $\mathbf{g}^{(2)}$ are obtained by perturbation theory.

Figure 2 shows maps of the angles α_1 *(a)*, α_2 *(b)*, $\tilde{\alpha}_1$ *(c)* and $\tilde{\alpha}_2$ *(d)* for the orthorombic medium. Each point on the maps represents a ray direction. The magnitude of the angles are shown by a grayscale: The larger the magnitude of the angle, the darker it is presented. One can see that the angles do not exceed 15 degrees (white and light-gray) for most rays. The largest angles (nearly black) correspond to singular directions of the orthorombic medium considered where the two shear wavefronts cross each other. In these directions the perturbation theory fails as well as the standard anisotropic ray theory. Therefore, these directions have to be excluded from our consideration. Comparison of the two upper *(a,b)* and the lower *(c,d)* maps shows that the angles $\tilde{\alpha}_1$ and $\tilde{\alpha}_2$ between the vectors $\tilde{\mathbf{g}}^{(1)}$ and $\tilde{\mathbf{g}}^{(2)}$ obtained by projection of the polarization vectors, $\mathbf{A}_{qS1}$ and $\mathbf{A}_{qS2}$, and the exact vectors $\mathbf{g}^{(1)}$ and $\mathbf{g}^{(2)}$ are smaller than the corresponding angles α_1 and α_2 between the polarization vectors $\mathbf{A}_{qS1}$ and $\mathbf{A}_{qS2}$ and the vectors $\mathbf{g}^{(1)}$ and $\mathbf{g}^{(2)}$.

Figure 3 shows similar maps of the angles α_1 *(a)*, α_2 *(b)*, $\tilde{\alpha}_1$ *(c)* and $\tilde{\alpha}_2$ *(d)* for the VTI medium. As in the previous case, the largest angles (dark) correspond to the singular directions of the VTI medium considered. There, qSV- and SH-wavefronts are tangent to each other around $\theta \approx 0^\circ$ and cross each other around $\theta \approx 60^\circ$. In the case of qSV-waves, the projections $\tilde{\mathbf{g}}^{(1)}$ of the polarization vectors $\mathbf{A}_{qSV}$ provide a better approximation of $\mathbf{g}^{(1)}$. The angles are smaller on map *(c)* in comparison with map *(a)*. The SH-wave polarization vectors, $\mathbf{A}_{SH}$, are already situated in the plane orthogonal to the reference ray. Therefore, projection does not improve the approximation of $\tilde{\mathbf{g}}^{(2)}$ (see maps *(b)* and *(d)*).

According to Figures 2 and 3 the angular deviations between $\tilde{\mathbf{g}}^{(1)}$ and $\tilde{\mathbf{g}}^{(2)}$ estimated from the qS-wave polarization vectors and the exact $\mathbf{g}^{(1)}$ and $\mathbf{g}^{(2)}$ vary from 0 till 15 degrees for the regular (non-singular) areas. The maximum deviation outside singular regions does not exceed 5 degrees for the VTI medium and 15 degrees for the orthorombic medium.

RECURRENT INVERSION SCHEME

In inhomogeneous anisotropic models the elastic parameters vary from one point in space to the other. The isotropic background model also becomes inhomogeneous. As a result the vectors $\mathbf{g}^{(1)}$ and $\mathbf{g}^{(2)}$ rotate along the reference ray due to two reasons: (1) inhomogeneity of the isotropic background medium, and

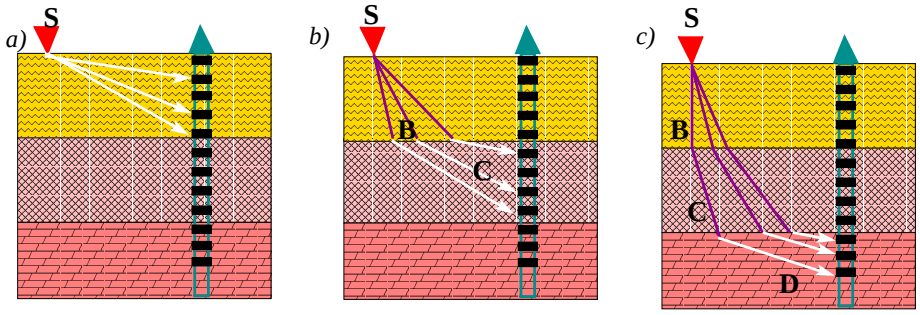

Figure 4: Recurrent inversion scheme: The model consists of three layers. The inversion procedure is performed in a layer-by-layer manner. *(a)* The perturbations Δa_{iklm} in the first layer are inverted using the observed data at the receivers situated in the first layer. *(b)* Traveltimes along the rays in the first layer are subtracted from the traveltimes observed at the receivers situated in the second layer. Then, these newly obtained traveltimes are used for inverting for Δa_{iklm} in the second layer. *(c)* To invert Δa_{iklm} in the third layer, traveltimes along the rays in the first and second layers are subtracted from the observed traveltimes.

(2) changes of the anisotropic parameters along the reference ray. To estimate the vectors $\mathbf{g}^{(1)}$ and $\mathbf{g}^{(2)}$, the observations of the polarization vectors $\mathbf{A}_{qS1}$ and $\mathbf{A}_{qS2}$ at each point along the reference ray would be needed. But the information about the polarization vectors $\mathbf{A}_{qS1}$ and $\mathbf{A}_{qS2}$ is available only at the receiver points. In the general case of inhomogeneity, this is not sufficient. But there are two types of inhomogeneous models, where the suggested inversion procedure can be applied.

The first type concerns media, where the rotations of the vectors $\mathbf{g}^{(1)}$ and $\mathbf{g}^{(2)}$ along the ray are initiated only by inhomogeneities of the isotropic background medium. An example of a such medium is the factorized anisotropic inhomogeneous (FAI) medium suggested by Červený and Simões-Filho (1991). In the FAI media, the rotations of the vectors $\mathbf{g}^{(1)}$ and $\mathbf{g}^{(2)}$ along the ray in the background medium are caused only by the inhomogeneity of the background medium. Therefore, the vectors $\mathbf{g}^{(1)}$ and $\mathbf{g}^{(2)}$ along the reference ray can be obtained by the standard isotropic ray method.

The second type consists of piecewise homogeneous anisotropic media. Piecewise homogeneous media are common in exploration seismics. For these media a recurrent inversion procedure can be suggested. To obtain the elastic parameters of an anisotropic layered model the inversion procedure described above can be applied recurrently. The model structure is supposed to be known, i.e., a VSP experiment is assumed. This means that the number of the layers and their depths are known. All receivers are divided into K groups, where K is the number of layers in the model considered. The inversion procedure is performed in K steps in a layer-by-layer manner. Figure 4 explains the procedure for an example of a three-layers model.

To estimate the elastic parameters of the first layer, only the observed data at the receivers situated in the first layer is used ($K = 1$). Since the layer is homogeneous, its elastic parameters are determined as described above. For the following steps the elastic parameters of the first layer and the corresponding background isotropic medium are assumed to be known from the inversion.

In the second step, data observed at the receivers from the second layer is used ($K = 2$). The reference ray paths in the isotropic background medium obtained for all waves recorded at these receivers consist of two parts (see Fig. 4*b*) those in the first layer (*SB*) and in the second layer (*BC*). The traveltime τ of each wave thus consists of two terms

$$\tau = \tau^{(I)} + \tau^{(II)},$$

where $\tau^{(I)}$ is the traveltime in the first layer and $\tau^{(II)}$ is the traveltime in the second layer. With the known elastic parameters of the first layer, the traveltimes $\tau^{(I)}$ in the first layer can easily be calculated by the equations (3) with the perturbation method. Then, the calculated traveltime $\tau^{(I)}$ is subtracted from the whole traveltime τ recorded at the receiver. As a result the traveltime $\tau^{(II)}$ along the ray path *BC* in the second layer is obtained. The second layer is homogeneous, therefore, the polarization vector at the receiver can be used to estimate the corresponding vector $\tilde{\mathbf{g}}^{(M)}$ along the ray path *BC*. With the traveltime $\tau^{(II)}$ and the vector $\tilde{\mathbf{g}}^{(M)}$ as input data, the inversion of the perturbations Δa_{iklm} in the second layer can

be performed in the same manner as in the first layer. Note that the parameters of the isotropic background medium in the first layer are fixed, whereas the parameters of the isotropic background medium in the second layer are searched with the help of the iteration procedure described above. Therefore, the reference ray paths have to be recalculate as soon as the parameters of the isotropic background medium in the second layer are changed.

In a similar way the elastic parameters of the third layer can be determined, see Fig. 4*c*. Now, the elastic parameters of the first and second layer are assumed to be known. Therefore, the traveltimes along the path in the first (*SB*) and second (*BC*) layers can be calculated. Then, the calculated traveltimes are subtracted from the observed traveltimes at the receivers of the third layer. The newly obtained traveltimes and polarization vectors at the receivers of the third layer are used to invert for the perturbations Δa_{iklm} in the third layer. Note that the parameters of isotropic background media in the first and second layers are known from the previous steps. Therefore, the iteration procedure for the construction of the isotropic background medium is only applied for the third layer.

In conclusions, the elastic parameters of all layers can be determined in the layer-by-layer manner using the already known elastic parameters of the upper layers and the observed traveltimes and polarization vectors in the layers under consideration.

CASE STUDY FOR THE THREE LAYER MODEL

A layered model was used to test the suggested recurrent inversion procedure. The model consists of three layers. The first layer is an anisotropic medium with orthorombic symmetry, the second layer is a transversely isotropic medium with vertical axis of symmetry (VTI). The density-normalized elastic parameters (in km^2/s^2) of the anisotropic layers are given in Table. 1 (see columns with A_{ik}^{true}). The third layer is isotropic and the P- and S-wave velocities are $V_p = 3.87\,\mathrm{km/s}$ and $V_s = 2.24\,\mathrm{km/s}$.

As observed data we used traveltimes and polarization vectors computed by the ANRAY package (see Gajewski and Pšenčík, 1990) in a synthetic vertical seismic profiling (VSP) experiment. The scheme of the VSP experiment is shown in Figure 5. A vertical borehole contains 25 aligned three-component receivers with 30 m vertical spacing until a depth of 750 m. There are 10 receivers in the first layer, 11 receivers in the second layer and 4 in the third isotropic layer. The receivers record the wavefields from 12 sources situated around the borehole on the Earth surface. In Figure 5 these 12 source positions are denoted by triangles. All sources are vertical forces.

According to the anisotropic ray theory, three waves arrive at each receiver in the first layer: one qP and two quasi-shear waves. Therefore, for each receiver in the first layer there are three traveltimes (qP, $qS1$ and $qS2$ waves). On the interface between two anisotropic layers each quasi-shear wave produces two quasi-shear waves. One wave is the same type as the incident wave, the other is a converted wave. Therefore, two incident quasi-shear waves produce four quasi-shear waves in the second layer ($qS1$-$qS1$, $qS2$-$qS2$, $qS1$-$qS2$ and $qS2$-$qS1$). As a result for each receiver in the second layer there is one qP-wave traveltime and four quasi-shear wave traveltimes. The converted $qP - qS$ and $qS - qP$ waves are not considered. Since the third layer is isotropic, there is one qP-wave traveltime and four qS-wave traveltimes.

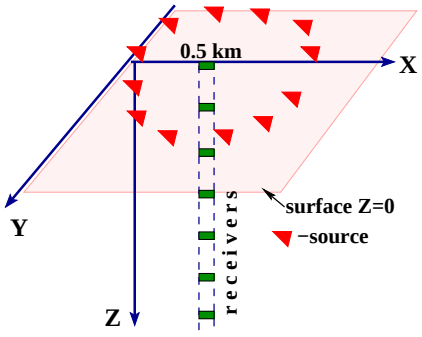

Figure 5: A vertical borehole contains 25 aligned three-component receivers with 30 m vertical spacing until a depth of 750 m. All sources are vertical forces. The 12 source positions are denoted by triangles.

INVERSION FOR THE FIRST LAYER

Inversion of the elastic parameters of the first layer is performed just as it is performed in homogeneous anisotropic media. The observed data from the first 10 receivers is used. There are 120 observations of qP-wave traveltimes, 120 and 115 observations of traveltimes and polarization vectors of $qS1$- and $qS2$-waves respectively. (Note that here and in the subsequent discussions the different number of observations of qP- and qS-waves is due to the excluding of some observations from the inversion. No observations were obtained for regions where the ray theory fails, e.g. for singular directions or for receivers situated closely to an interface.) Noise is added to the synthetic traveltimes and qS-wave polarization vectors. The noisy data have a standard deviation of 2 ms for the traveltimes and a standard deviation of 10° for the inclination (α) and the azimuth (β) angles specifying the qS-wave polarization vectors. The final isotropic background medium has $v_p = 3.14$ and $v_s = 1.99$ km/s.

Let us assume that there is no a priori knowledge on the type of anisotropy. Therefore, an inversion for all 21 elastic parameters must be performed. The results of the inversion are given in the third column of Table 1*(a)*. The misfit function η^2 is 0.0013 s^2. Since the condition number (ration of the maximal singular value to the minimal singular value) of the SVD was 28, the inversion problem for 21 parameters was well conditioned. Therefore all inverted parameters are acceptable. The inverted parameters are close to the exact ones. The RMSD of the inverted parameters, $A_{ik}^{\rm est}(21)$ from the exact parameters, $A_{ik}^{\rm true}$, is 2.46%.

For each inverted parameter, we obtained also a confidence interval with a probability coefficient of 99%. The non-orthorombic parameters of $A_{ik}^{\rm est}(21)$ are relatively small. The corresponding confidence intervals show that these small parameters can not be distinguished from zero. Therefore, we can conclude about the orthorombic symmetry of the considered medium. In this case we can restrict the inversion to nine independent elastic parameters: A_{11}, A_{12}, A_{13}, A_{22}, A_{23}, A_{33}, A_{44}, A_{55} and A_{66}. The results of the inversion for the 9 parameters are given in the fourth column of Table 1*(a)*. The inverted parameters $A_{ik}^{\rm est}(9)$ are given with the confidence intervals of 99% probability ($I_{99\%}$). The misfit function η^2 equals to 0.0013 s^2. The RMSD of the inverted parameters $A_{ik}^{\rm est}(9)$ from the exact parameters, $A_{ik}^{\rm true}$, is 2.41%. Note that the inversion problem for 9 parameters was well conditioned, because the condition number of the SVD was 28.

What happens if we ignore that the medium under consideration is an anisotropic medium? Figure 6 shows traveltime residuals for the first layer obtained after the inversion of noise-free data for the 9 elastic parameters (crosses) and after the inversion for only 2 parameters (isotropic P- and S-wave velocities) (stars). The traveltime residuals are given in ms. One can see that the traveltimes for the inverted anisotropic medium differ from the observed traveltimes by only 1-3 ms for the qP- as well as for the two quasi-shear waves. The deviations of the isotropic traveltimes, however, are as big as 10-15 ms.

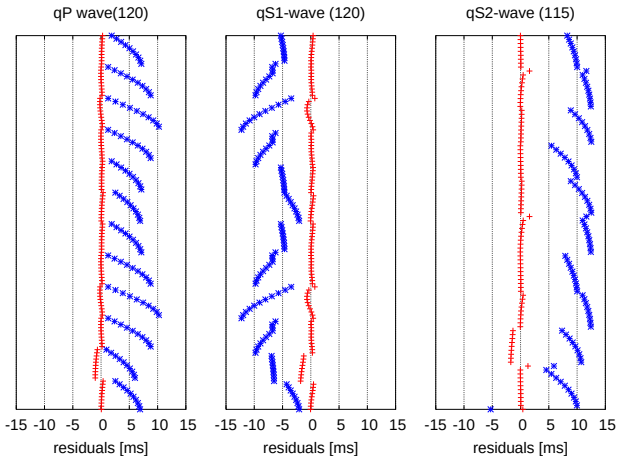

Figure 6: Traveltime residuals after inversion of noise-free data in the first orthorombic layer. Crosses show traveltime residuals after inversion for 9 different elastic parameters defining the orthorombic medium, stars show the traveltime residuals after inversion for 2 isotropic parameters. 120 observations of the qP-wave traveltimes, 120 and 115 observations of $qS1$- and $qS2$-waves, respectively, were used.

INVERSION FOR THE SECOND LAYER

In the second layer there are 11 receivers. The data includes 132 observations of qP-waves, 131 and 109 observations respectively of $qS1 - qS1$- and $qS1 - qS2$-waves, 128 and 117 observations respectively of

a)

First layer, σ_t=2ms, σ_α=10°, σ_β=10°					
	A_{ik}^{true}	$A_{ik}^{\text{est}}(21)$	$I_{99\%}$	$A_{ik}^{\text{est}}(9)$	$I_{99\%}$
A_{11}	10.800	10.658	±0.132	10.656	±0.130
A_{12}	2.200	2.152	±0.102	2.153	±0.101
A_{13}	1.900	1.797	±0.254	1.797	±0.251
A_{14}	0.	0.003	±0.097	0.	
A_{15}	0.	0.009	±0.066	0.	
A_{16}	0.	0.000	±0.052	0.	
A_{22}	11.300	11.080	±0.130	11.080	±0.129
A_{23}	1.700	1.722	±0.255	1.722	±0.252
A_{24}	0.	0.023	±0.067	0.	
A_{25}	0.	-0.004	±0.081	0.	
A_{26}	0.	-0.001	±0.050	0.	
A_{33}	8.500	8.050	±0.571	8.052	±0.563
A_{34}	0.	0.029	±0.071	0.	
A_{35}	0.	0.021	±0.074	0.	
A_{36}	0.	0.008	±0.084	0.	
A_{44}	3.600	3.550	±0.040	3.550	±0.040
A_{45}	0.	0.006	±0.032	0.	
A_{46}	0.	-0.004	±0.036	0.	
A_{55}	3.900	3.886	±0.040	3.886	±0.039
A_{56}	0.	0.004	±0.039	0.	
A_{66}	4.300	4.315	±0.028	4.314	±0.027

b)

Second layer, σ_t=3ms, σ_α=15°, σ_β=15°							
	A_{ik}^{true}	$A_{ik}^{\text{est}}(21)$	$I_{99\%}$	$A_{ik}^{\text{est}}(9)$	$I_{99\%}$	$A_{ik}^{\text{est}}(5)$	$I_{99\%}$
A_{11}	13.590	13.611	±1.237	13.601	±1.236	14.173	±1.270
A_{12}	6.800	6.836	±1.155	6.844	±1.153	5.919	±0.247
A_{13}	5.440	5.576	±0.453	5.568	±0.452	5.599	±0.396
A_{14}	0.	0.057	±0.200	0.		0.	
A_{15}	0.	-0.111	±0.182	0.		0.	
A_{16}	0.	-0.047	±0.314	0.		0.	
A_{22}	13.590	13.657	±1.240	13.643	±1.238	14.173	±1.270
A_{23}	5.440	5.428	±0.455	5.420	±0.453	5.599	±0.396
A_{24}	0.	0.121	±0.181	0.		0.	
A_{25}	0.	-0.103	±0.200	0.		0.	
A_{26}	0.	0.014	±0.311	0.		0.	
A_{33}	10.870	10.436	±1.306	10.421	±1.303	10.338	±1.538
A_{34}	0.	-0.036	±0.184	0.		0.	
A_{35}	0.	-0.076	±0.185	0.		0.	
A_{36}	0.	-0.065	±0.315	0.		0.	
A_{44}	4.100	4.050	±0.249	4.061	±0.245	4.069	±0.273
A_{45}	0.	-0.006	±0.094	0.		0.	
A_{46}	0.	-0.014	±0.068	0.		0.	
A_{55}	4.100	4.107	±0.247	4.117	±0.245	4.069	±0.273
A_{56}	0.	-0.006	±0.061	0.		0.	
A_{66}	4.500	4.576	±0.285	4.577	±0.284	4.127	±0.322

Table 1: Results of the inversion of two layers of the three layered model. The first layer is an orthorombic medium *(a)*; the second layer is a VTI medium *(b)*. The true elastic parameters are given in the columns A_{ik}^{true}. Random noise with a normal probability distribution is added into the synthetic traveltimes and polarization vectors. The standard deviation for the traveltimes is denoted as σ_t and for the inclination (α) and azimuth (β) angles defined the qS-wave polarization vectors as σ_α and σ_β. For the orthorombic medium the inversion of the noisy data was performed for 21 and 9 parameters (see $A_{ik}^{\text{est}}(21)$ and $A_{ik}^{\text{est}}(9)$). For the VTI medium the inversion of the noise data was performed for 21, 9 and 5 parameters (see $A_{ik}^{\text{est}}(21)$, $A_{ik}^{\text{est}}(9)$ and $A_{ik}^{\text{est}}(5)$). For each estimated parameter the confidence interval with 99% probability (denoted by $I_{99\%}$) is given.

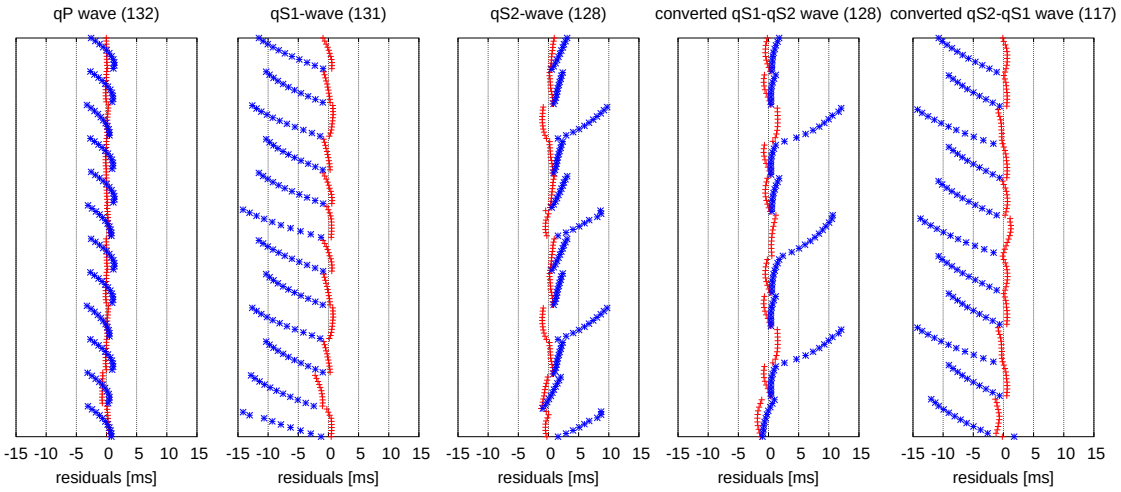

Figure 7: Traveltime residuals after the inversion of noise-free data in the second VTI layer. Crosses show traveltime residuals after the inversion for 5 elastic parameters defining the VTI medium, stars show the traveltime residuals after the inversion for 2 isotropic elastic parameters.

$qS2-qS1$- and $qS2-qS2$-waves. As in the previous examples, noise is added to the synthetic traveltimes and qS-wave polarization vectors. The noisy data has a standard deviation of 3 ms for the traveltimes and a standard deviation of 15° for the inclination (α) and azimuth (β) angles specifying the qS-wave polarization vectors. The final isotropic background medium has $v_p = 3.65$ km/s and $v_s = 1.97$ km/s.

If there is no a priori knowledge on the type of anisotropy, the inversion must be performed for all 21 elastic parameters. The results of the inversion are given in Table 1*(b)*. For each inverted parameter, a confidence interval with a probability coefficient of 99% is given. The misfit function η^2 is 0.0060 s^2. Since the condition number of the SVD was 37, the inversion problem for 21 parameters was well conditioned. Therefore all inverted parameters are acceptable.

The confidence intervals show that the small non-orthorombic inverted parameters of $A_{ik}^{\rm est}(21)$ can not be distinguished from zero. One can conclude that the considered medium possesses orthorombic symmetry or VTI symmetry. The last two columns of Table 1*(b)* give the results of the inversion for 9 parameters, $A_{ik}^{\rm est}(9)$, and for 5 parameters, $A_{ik}^{\rm est}(5)$. The misfit function η^2 is 0.0061 s^2 in the first case and 0.0086 s^2 in the last case. Note that the condition numbers of the SVD was 35 for the inversion for 9 parameters and 37 for the inversion for 5 parameters. Therefore, all 9 or 5 inverted parameters are acceptable. For each inverted parameter the corresponding confidence interval is obtained. Analysis of these confident interval shows that the inverted parameters $A_{ik}^{\rm est}(9)$ can not be distinguished from the inverted parameters $A_{ik}^{\rm est}(5)$. Please note that among the inverted parameters $A_{ik}^{\rm est}(9)$, the parameter A_{11} can not be distinguished from the parameter A_{22}, A_{44} from A_{55} and A_{13} from A_{23}. This means that the medium of the second layer possesses most likely VTI symmetry. The RMSD of the inverted parameters $A_{ik}^{\rm est}(5)$ from the exact parameters $A_{ik}^{\rm true}$ is 5.9%.

What happens if we ignore that the medium under consideration is anisotropic medium? Figure 7 shows traveltime residuals obtained after the inversion of noise-free data for the 5 elastic parameters (crosses) and after the inversion for only 2 parameters (isotropic P- and S-wave velocities) (stars). Traveltime residuals are given in ms. One can see that the traveltimes for the inverted anisotropic medium differ from the observed traveltimes by 1–3 ms for the qP- as well as for the two quasi-shear waves. The deviations of the isotropic traveltimes, however, are as big as 10–15 ms.

INVERSION FOR THE THIRD LAYER

In the third layers 4 receivers are situated. There are 36 observations of the P-waves and 133 observations of S-waves. According to the discussion on page 337, the observations of the S-waves are separated into four groups: $qS1-qS1-S$ (35 observations), $qS2-qS2-S$ (31), $qS1-qS2-S$ (34) and

$qS2 - qS1 - S$ (33). Noise is added to the traveltimes and qS-wave polarization vectors. The noisy data has a standared deviation of 3 ms for the traveltimes and standard deviations of 15° for the inclination (α) and azimuth (β) angles specifying the qS-wave polarization vectors. The inversion was performed for 2 parameters (the square of P- and S-wave velocities, V_p^2 and V_s^2). The misfit function η^2 was 0.0014 s^2. The condition number of the SVD was 10. As a result the following P- and S-wave velocities and their confidence intervals with a probability coefficient of 99% were obtained:

$$V_p^2 = 4.03\,\mathrm{km/s} \quad I_{99\%} = 1.30$$
$$V_s^2 = 2.26\,\mathrm{km/s} \quad I_{99\%} = 0.44$$

(The exact velocities of the third layer are $V_p = 3.87$ km/s and $V_s = 2.24$ km/s.)
Figure 8 shows traveltime residuals in the third isotropic layer after the inversion of noise-free data for 2 parameters. The residuals are 1–3 ms

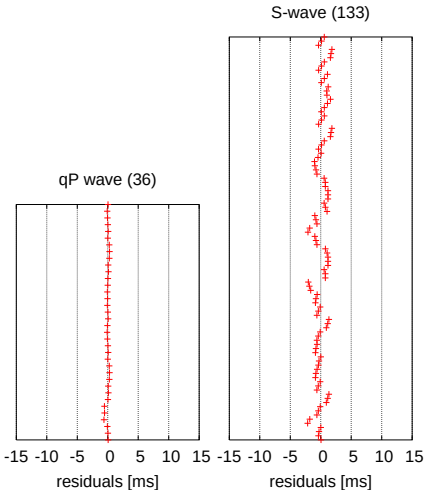

Figure 8: Traveltime residuals after the inversion of noise-free data in the third isotropic layer. Crosses show traveltime residuals after inversion for the isotropic elastic parameters.

CONCLUSIONS

An inversion procedure for weakly anisotropic media using traveltimes of qP- and qS-waves as well as qS-wave polarizations was suggested. The presented inversion procedure allows to use the same linear inversion scheme for qP- as well as for qS-wave data. The joint inversion of qP- and qS-waves allows to determine the full elastic tensor of the anisotropic medium.

The advantage of the presented inversion procedure is that no assumption about any special type of anisotropic symmetry is needed. If there is no a priori information on the type of anisotropy, all 21 elastic parameters can be inverted. Then, analysis of the 21 inverted elastic parameters can be carried out. Based upon the significance and accuracy of each parameter, we can restrict the inversion to a smaller number of the elastic parameters and determine the symmetry of the media under consideration.

The main restriction of the suggested inversion procedure is that it is based on perturbation theory which provides a smooth transition from isotropic media to anisotropic media by small perturbations of the elastic parameters. Therefore, the accuracy of the traveltime computations in the forward modeling problem and, as a result, the quality of the inversion depend directly on the assumption of weak anisotropy. This means that the inversion procedure allows to reconstruct the exact elastic parameters only if the anisotropic medium is weakly anisotropic. In the case of the medium with more then 5% anisotropy, the inversion does not reconstruct the exact elastic parameters, but only gives close estimates of these elastic parameters even when the noise-free data are used. But note that because the inversion procedure can be performed fast and has no restrictions on the types of anisotropic symmetry, it can be used to construct initial models for non-linear inversion procedures.

In comparison to a conventional tomography scheme, the suggested inversion scheme requires not only traveltime observations, but also the observed qS-wave polarization vectors. Although the observed qS-wave polarizations are available from three component data, picking qS-wave polarization vectors from real data can be a challenging task. However, to obtain traveltimes, the two qS-waves need to be separated in any case. For this separation the difference in qS-wave polarizations is used (see, e.g., Alford, 1986; Li and Crampin, 1993; Dellinger et al., 1998). Therefore, the qS-wave polarization vectors are automatically obtained as a by-product of the qS-wave separation.

For layered models the inversion can be applied in a layer-by-layer manner (recurrently). The recurrent inversion was tested on a model consisting of three layers: The first layer was an anisotropic medium

with orthorombic symmetry (10.6% anisotropy), the second layer was a medium with VSP symmetry (11% anisotropy) and the third layer was an isotropic medium. Synthetic qP- and qS-wave traveltimes and qS-wave polarization vectors were generated for a VSP experiment by the ANRAY program package (Gajewski and Pšenčík, 1987). Noisy data was used for the inversion. Errors were introduced in the qP- and qS-wave traveltimes as well as in the qS-wave polarization vectors. The RMSD of the inverted elastic parameters from the exact parameters were 2.41% for the first orthorombic layer, 5.9% for the second VTI layer, and 10% for the third isotropic layer. For each inverted parameter a confidence interval with a probability coefficient of 99% was constructed. The values of the traveltimes residuals varied from 1–3 ms. These correspond to errors in picking of traveltimes of the different waves from real data.

ACKNOWLEDGMENTS

This research was partly supported by the German Research Foundation (DFG Ga 350/11-1), the sponsors of the Wave Inversion Technology (WIT) Consortium, the German Academic Exchange Service (DAAD) and the Russian Foundation of Fundamental Research. We are grateful to the members of the Applied Geophysics Group for useful discussions and the improvement of the manuscript.

REFERENCES

Alford, R. M. (1986). Shear data in the presence of azimuthal anisotropy. In *Expanded Abstracts*, page S9.6. Soc. Expl. Geophys.

Červený, V. (1982). Direct and inverse kinematic problems for inhomogeneous anisotropic media – a linearization approach. *Contr. Geophys. Inst. Sov. Acad. Sci.*, 13:127–133.

Červený, V. (2001). *Seismic ray theory*. Cambridge University Press.

Červený, V. and Jech, J. (1982). Linearized solutions of kinematic problems of seismic body waves in inhomogeneous slightly anisotropic media. *Geophys. J. Int*, 51:96–104.

Červený, V. and Simões-Filho, I. A. (1991). The traveltime perturbations for seismic body waves in factorized anisotropic inhomogeneous media. *Geophys. J. Int*, 107:219–229.

Chapman, C. H. and Pratt, R. G. (1992). Traveltime tomography in anisotropic media — I. Theory. *Geophys. J. Int*, 109:1–19.

Cliet, C., Brodov, L., Tikhonov, A., Marin, D., and Michon, D. (1991). Anisotropy survey for reservoir definition. *Geophys. J. Int*, 107:417–427.

Dellinger, J., Nolte, B., and Etgen, J. (1998). Symmetric Alford diagonalization. In *Expanded Abstracts*, pages 1673–1676. Soc. Expl. Geophys.

Farra, V. and Le Bégat, S. (1995). Sensitivity of qP-wave traveltimes and polarization vectors to heterogeneity, anisotropy and interfaces. *Geophys. J. Int.*, 121:371–384.

Fedorov, F. I. (1968). *Theory of elastic waves in crystals*. Plenum Press, New York.

Gajewski, D. and Pšenčík, I. (1987). Computation of hight-frequency seismic wavefields in 3-D laterally inhomogeneous anisotropic media. *Geophys. J. R. astr. Soc.*, 91:383–411.

Gajewski, D. and Pšenčík, I. (1990). Vertical seismic profile synthetics by dynamic tracing in laterally varying layered anisotropic structures. *J.Geophys.Res.*, 95:11301–11315.

Horne, S. and Leaney, S. (2000). Short note: Polarization and slowness component inversion for TI anisotropy. *Geophysical Prospecting*, 48:779–788.

Horne, S. and MacBeth, C. (1994). Inversion for seismic anisotropy using genetic algorithms. *Geophysical Prospecting*, 42:953–974.

Jech, J. and Pšenčík, I. (1989). First-order perturbation method for anisotropic media. *Geophys. J. Int*, 99:369–376.

Jech, J. and Pšenčík, I. (1992). Kinematic inversion for qP and qS waves in inhomogeneous hexagonally symmetric structures. *Geophys. J. Int*, 108:604–612.

Le Bégat, S. and Farra, V. (1997). P-wave traveltime and polarization tomography of VSP data. *Geophys. J. Int.*, 131:100–114.

Li, X. Y. and Crampin, S. (1993). Linear-transform techniques for processing shear-wave anisotropy in four-component seismic date. *Geophysics*, 58:240–256.

Linnik, Y. V. (1961). *Method of least squares and principles of the theory of observations*. Pergamon Press.

Menke, W. (1984). *Geophysical data analysis: discrete inverse theory*. Academic Press, Inc.

Williamson, P. R. (1993). Anisotropic crosshole tomography in layered media. Part II: applications, results and conclusions. *Journ. Seismic. Explor.*, 2:223–238.